Citation: Cell Death and Disease (2010) 1, e50; doi:10.1038/cddis.2010.28

www.nature.com/cddis

IGF1 activates cell cycle arrest following irradiation by reducing binding of ΔNp63 to the p21 promoter

GC Mitchell[1], JL Fillinger[2], S Sittadjody[2], JL Avila[3], R Burd[2] and KH Limesand*[,1,2,3]

Radiotherapy for head and neck tumors often results in persistent loss of function in salivary glands. Patients suffering from impaired salivary function frequently terminate treatment prematurely because of reduced quality of life caused by malnutrition and other debilitating side-effects. It has been previously shown in mice expressing a constitutively active form of Akt (myr-Akt1), or in mice pretreated with IGF1, apoptosis is suppressed, which correlates with maintained salivary gland function measured by stimulated salivary flow. Induction of cell cycle arrest may be important for this protection by allowing cells time for DNA repair. We have observed increased accumulation of cells in G2/M at acute time-points after irradiation in parotid glands of mice receiving pretreatment with IGF1. As p21, a transcriptional target of the p53 family, is necessary for maintaining G2/M arrest, we analyzed the roles of p53 and p63 in modulating IGF1-stimulated p21 expression. Pretreatment with IGF1 reduces binding of ΔNp63 to the p21 promoter after irradiation, which coincides with increased p53 binding and sustained p21 transcription. Our data indicate a role for ΔNp63 in modulating p53-dependent gene expression and influencing whether a cell death or cell cycle arrest program is initiated.

Cell Death and Disease (2010) **1,** e50; doi:10.1038/cddis.2010.28; published online 10 June 2010
Subject Category: Cancer

Over 50 000 cases of head and neck cancer are expected to be reported in the United States in 2010.[1] For these cancers, radiation therapy is a common treatment modality, but irradiation of this region often results in secondary side-effects in non-diseased tissues, including drastic loss of salivary gland function. This reduction in salivary flow leads to xerostomia, or chronic dry mouth, which can have a profound effect on a patient's quality of life. Those affected have difficulty speaking, chewing and swallowing, and often suffer from malnutrition.[2] To minimize these complications, clinicians attempt to limit the dose of therapeutic radiation reaching the parotid gland to 1.8–2 Gy fractions totaling no more than 26 Gy over the course of treatment.[3] However, on the basis of tumor location and lymph node involvement, sparing of salivary glands may not be possible, with higher radiation doses resulting in permanent loss of function.

On DNA damage, the molecular sensors ATM (ataxia telangiectasia mutated) and ATR (ATM and Rad3-related) phosphorylate p53 at Ser^{15}.[4–6] It has been suggested that phosphorylation at this site is required for p53 stability in response to ionizing radiation.[7] Stabilized p53 can then transactivate genes involved in cell death, cell cycle arrest and DNA repair.[8] The response of a particular cell type or tissue to DNA damage likely depends on which of these programs is initiated by p53. We have previously shown a dose-dependent loss of salivary acinar cells to p53-dependent apoptosis after irradiation of mice, which coincides with a reduction in glandular function.[9] In addition, activation of endogenous Akt by IGF1 suppresses DNA damage-induced apoptosis in a parotid acinar cell line (C5) as well as in primary cultures of enriched acinar cells.

Although p53-dependent apoptosis has been extensively studied, identification of p53 homologs (p63 and p73) has added additional complexity to the understanding of how apoptosis is regulated. Transcription from alternate promoters results in two groups of p63 isoforms – full-length proteins containing a transactivation domain (TAp63) and truncated proteins lacking this domain (ΔNp63).[10] As a result of alternative splicing, each of these groups consists of three isoforms (α, β and γ). In general, the TA isoforms function similarly to p53, whereas the ΔN isoforms antagonize TAp63 as well as p53. Studies in several cell lines have shown that ΔNp63α can bind to p53 response elements, leading to reduced expression of genes such as MDM2, IGFBP-3 and p21.[11–13]

In this study, we show that parotid glands of mice pretreated with intravenous IGF1 before head and neck irradiation exhibit increased G2/M arrest compared with glands of mice treated with radiation alone. This coincides with sustained expression of p21 and elevated levels of cdc2 (Tyr^{15}) phosphorylation, which are known G2/M checkpoint regulators.[14] We also show that IGF1-induced cell cycle arrest is dependent on Akt and p53. Owing to a potential role for ΔNp63 in regulating p53 target genes, we performed chromatin immunoprecipitation

[1]Cancer Biology Graduate Interdisciplinary Program; [2]Department of Nutritional Sciences, University of Arizona, PO Box 210028, Tucson, Arizona 85721, USA and [3]Physiological Sciences Graduate Interdisciplinary Program
*Corresponding author: KH Limesand, Department of Nutritional Sciences, University of Arizona, 1177 E. 4th St., Shantz 421, Tucson, AZ 85721, USA.
Tel: 520 626 4517; Fax: 520 621 9446; E-mail: limesank@u.arizona.edu
Keywords: IGF1; p63; p53; radiation; cell cycle arrest; xerostomia
Abbreviations: IGF1, insulin-like growth factor 1; ATM, ataxia telangiectasia mutated; ATR, ATM and Rad3-related; MDM2, murine double minute 2; IGFBP-3, IGF binding protein-3; ChIP, chromatin immunoprecipitation; PCNA, proliferating cell nuclear antigen
Received 23.3.10; revised 30.4.10; accepted 12.5.10; Edited by G Melino

(ChIP) to evaluate p21 promoter occupancy at acute time-points in the glands of irradiated mice. Parotid glands of mice pretreated with IGF1 exhibit reduced binding of ΔNp63 to the p21 promoter, which corresponds to increased binding of p53, higher expression of p21 and G2/M arrest. Overall, our results suggest a role for ΔNp63 in directing p53 to initiate either a cell death or cell cycle arrest program. Insights into this mechanism may provide an important translational opportunity for development of small molecules to minimize side-effects of cancer therapies.

Results

Increased cell cycle arrest in irradiated parotid glands pretreated with IGF1. Radiation-induced DNA damage activates p53, which transactivates genes involved in cell death, cell cycle arrest and DNA repair.[8] We have previously shown that IGF1 activates endogenous Akt *in vivo* and suppresses radiation-induced apoptosis; this correlates with preservation of salivary gland function.[15] Studies *in vitro* have indicated that radiation can lead to accumulation of cells in G2/M, thereby reducing the S-phase population.[14] To examine this, single cell suspensions from treated parotid glands were stained with propidium iodide and analyzed by flow cytometry. Interestingly, radiation alone does not alter the percentage of cells in G2/M 8 h after treatment (Figure 1a). In contrast, cells isolated from parotid glands of mice pretreated with IGF1 have a fourfold increase in the G2/M population compared with untreated mice and a corresponding reduction in the percentage of S-phase cells (Figure 1b). To confirm that IGF1 induces arrest in irradiated salivary glands, we measured proliferation by staining tissue sections for proliferating cell nuclear antigen (PCNA). The percentage of PCNA-positive acinar cells after 24 h is unchanged in the glands of mice treated with radiation alone,

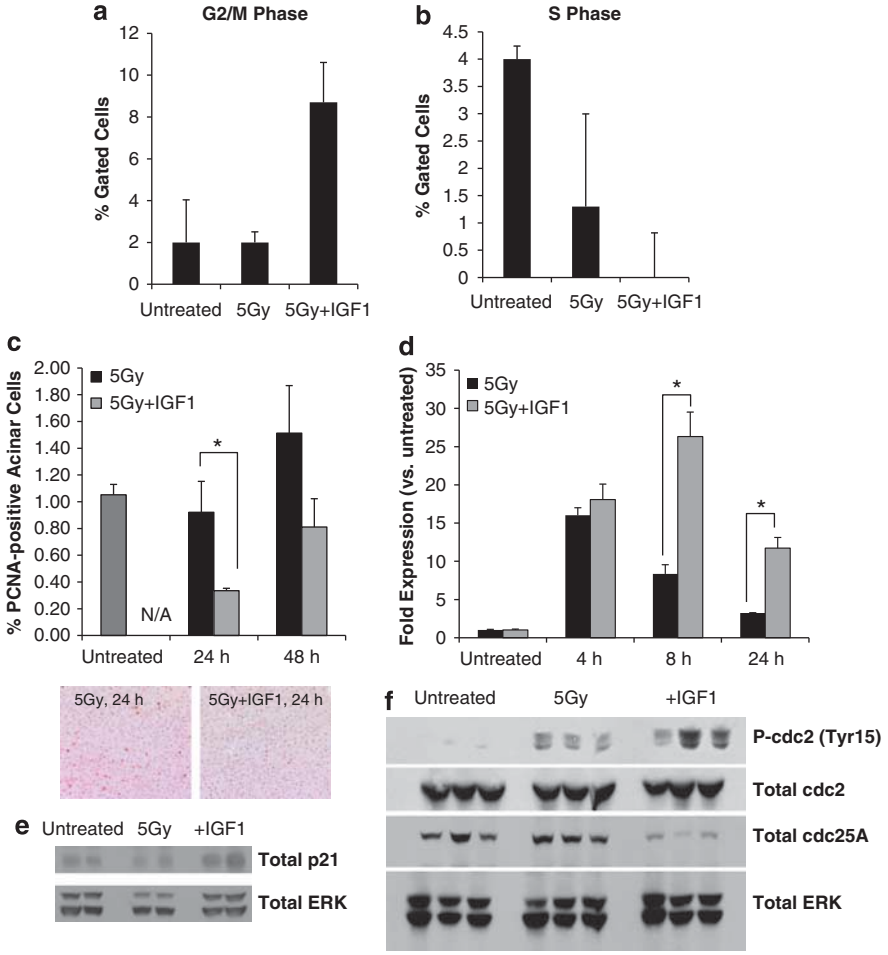

Figure 1 Pretreatment with IGF1 induces cycle arrest in irradiated parotid glands. The head and neck regions of wild-type mice were irradiated ± IGF1 pretreatment. Parotid glands were removed 4, 8, 24 and 48 h after treatment. (**a**, **b**) In all, 8 h tissues were dispersed, stained with propidium iodide and analyzed by flow cytometry. The data are shown as the mean percentage of gated cells in G2/M (**a**) or S phase (**b**) + S.E.M. of ⩾3 mice per treatment. (**c**) In total, 24 and 48 h tissues were embedded in paraffin and stained for PCNA. The graphs represent the number of PCNA-positive acinar cells as a percentage of total acinar cells counted. The data are shown as the mean + S.E.M. of ⩾3 mice per treatment. Representative PCNA images are shown below the graph. (**d**) RNA was isolated from 4, 8 and 24 h tissues, and real-time RT-PCR was run with primers to amplify total p63. Results were calculated using the $2^{-\Delta\Delta G_t}$ method, normalized to untreated and shown as the mean + S.E.M. of ⩾3 mice per treatment. (**e**, **f**) Protein lysates were prepared from 8 (**e**) and 6 h (**f**) tissues, and western blotting was performed as described in Materials and methods. Total ERK was used to confirm equal loading of lanes. *A significant difference ($P \leqslant 0.05$) between irradiated glands ± IGF1 pretreatment as measured by a Student's *t*-test

but decreases substantially in mice pretreated with IGF1 (Figure 1c). After 48 h, the percentage of PCNA-positive acinar cells in the glands of mice pretreated with IGF1 returns to untreated levels.

DNA damage-induced G2/M arrest depends on expression of p21, an inhibitor of the cyclin-dependent kinase cdc2.[14] To determine if IGF1-mediated G2/M arrest is facilitated by p21, we used real-time RT-PCR to look for differences in p21 expression in parotid glands of irradiated mice with and without IGF1 pretreatment. There is significantly higher p21 expression after 8 and 24 h in parotid glands of mice pretreated with IGF1 than in those treated with radiation alone (Figure 1d), which coincides with increased protein (Figure 1e). IGF1 pretreated mice receiving radiation also have elevated levels of phosphorylated cdc2 (Tyr^{15}) and decreased levels of the phosphatase cdc25A (Figure 1f), all of which indicate checkpoint activation. Collectively, these data suggest that IGF1 stimulation before irradiation induces an acute, transient G2/M arrest and may explain the reduced apoptotic phenotype and preserved physiological function we previously reported in IGF1 pretreated parotid glands.[15]

Increased cell cycle arrest in irradiated parotid glands of mice involves Akt. IGF1 is a potent activator of Akt in salivary acinar cells *in vitro* and *in vivo*.[15,16] We have previously described the phenotype of myr-Akt1 transgenic mice;[17] similar to mice injected with IGF1, myr-Akt1 mice have reduced radiation-induced apoptosis and preserved salivary gland function.[15] To determine the effect of constitutively active Akt (myr-Akt1) on radiation-induced G2/M arrest, we irradiated transgenic mice expressing a constitutively active form of Akt (myr-Akt1) and assessed cell cycle distribution as described above. Contrary to wild-type mice treated with radiation alone (Figure 1a), the parotid glands of irradiated myr-Akt1 mice have a larger G2/M population than untreated glands (Figure 2a). Similarly, these same glands have decreased proliferation measured by PCNA staining, 24 and 48 h after irradiation (Figure 2b). We also evaluated the effect of myr-Akt1 on p21 expression after irradiation. After 8 and 24 h, p21 expression increases significantly in parotid glands of myr-Akt1 mice treated with radiation, (Figure 2c). As cell cycle arrest in irradiated myr-Akt1 parotid glands is similar to the response in IGF1 pretreated

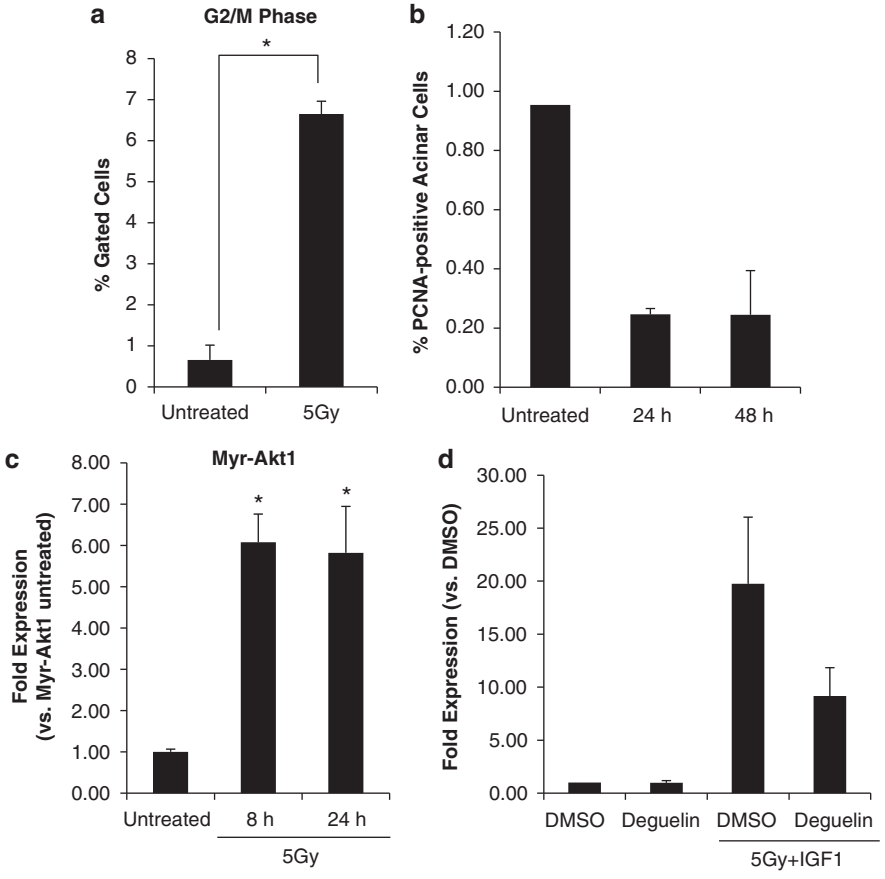

Figure 2 Radiation induces cell cycle arrest in myr-Akt1 mice. The head and neck regions of myr-Akt1 mice were irradiated (**a**–**c**). Parotid glands were removed 8, 24 and 48 h after treatment. (**a**) In all, 8 h tissues were dispersed, stained with propidium iodide and analyzed by flow cytometry. The data are shown as the mean percentage of gated cells in G2/M + S.E.M. of $\geqslant 3$ mice per treatment. (**b**) In total, 24 and 48 h tissues were embedded in paraffin and stained for PCNA. The graphs represent the number of PCNA-positive acinar cells as a percentage of total acinar cells counted. The data are shown as the mean + S.E.M. (**c**) RNA was isolated from 8 and 24 h tissues, and real-time RT-PCR was run with primers to amplify p21. Results were calculated using the $2^{-\Delta\Delta C_t}$ method, normalized to wild-type untreated and shown as the mean + S.E.M. of $\geqslant 3$ mice per treatment. *A significant difference ($P \leqslant 0.05$) between untreated and irradiated glands. (**d**) Wild-type mice were treated intraperitoneally with deguelin (4 mg/kg) immediately before IGF1 injections and head and neck irradiation. Parotid glands were removed after 8 h, RNA was isolated, and real-time RT-PCR was run with primers to amplify p21. Results were calculated using the $2^{-\Delta\Delta C_t}$ method, normalized to vehicle control (DMSO alone) and shown as the mean + S.D.

parotid glands, we assessed whether the effects of IGF1 were mediated through Akt activation using the Akt inhibitor deguelin. Pretreatment with deguelin reduces IGF1-induced p21 expression in irradiated parotid glands by roughly 50% (Figure 2d). These results imply that the IGF1-induced cell cycle arrest in irradiated parotid glands may involve Akt.

Sustained phosphorylation of p53 (Ser^{18}) in parotid glands of irradiated mice. In response to DNA damage, p53 undergoes a number of posttranslational modifications that increase its stability and transcriptional activity. It has been suggested that phosphorylation at Ser^{15} stabilizes p53 after irradiation, allowing for transactivation of p53 target genes.[7] Phosphorylation of the corresponding site in mice (Ser^{18}) also occurs in irradiated parotid glands.[17] We evaluated DNA damage-induced changes to p53 protein levels in parotid glands by probing for total and phosphorylated p53 (Ser^{18}). Although elevated over untreated, the level of phosphorylated p53 protein (Ser^{18}) is significantly reduced in IGF1 pretreated glands after 8 h compared with glands treated with radiation alone (Figures 3a and b). These results indicate that IGF1 reduces DNA damage-induced p53 phosphorylation and stabilization in parotid glands 8 h after irradiation.

Radiation-induced cycle arrest in parotid glands is dependent on p53. To assess whether or not IGF1-induced G2/M arrest is p53 dependent, we irradiated p53$^{-/-}$ mice with or without IGF1 pretreatment and stained parotid tissue for PCNA. After 24 h, the percentage of PCNA-positive acinar cells was unchanged in the glands of p53$^{-/-}$ mice treated with radiation alone (Figure 4a). In contrast to wild-type mice, the percentage of PCNA-positive acinar cells increases significantly in the glands of p53$^{-/-}$ mice pretreated with IGF1. Recent work from our lab showed that radiation-induced expression of two canonical p53 target genes, Bax and PUMA, is p53 dependent in parotid glands.[9] To confirm this relationship for another canonical p53 target gene, the cell cycle arrest gene p21, we used real-time RT-PCR to measure its transcription 4 h after irradiation in p53$^{+/+}$, p53$^{+/-}$ and p53$^{-/-}$ mice. In both p53$^{+/+}$ and p53$^{+/-}$ parotid glands, p21 increases significantly 4 h after irradiation compared with untreated glands from mice of the same genotype (Figure 4b). In p53$^{-/-}$ mice there is no induction of p21 after irradiation, showing that radiation-induced p21 transcription is p53 dependent.

To confirm that IGF1 affects p21 expression in a p53-dependent manner, we used real-time RT-PCR to measure p21 expression in p53$^{-/-}$ parotid glands 8 h after irradiation. Without functional p53, there is no increase in p21 transcription 8 h after irradiation (Figure 4c). We confirmed the requirement for p53 transcriptional activation in IGF1-mediated p21 expression using pifithrin-α. Pretreatment with pifithrin-α prevents the sustained p21 expression observed in parotid glands of mice pretreated with IGF1 (Figure 4d). These data show that IGF1-induced G2/M arrest in irradiated

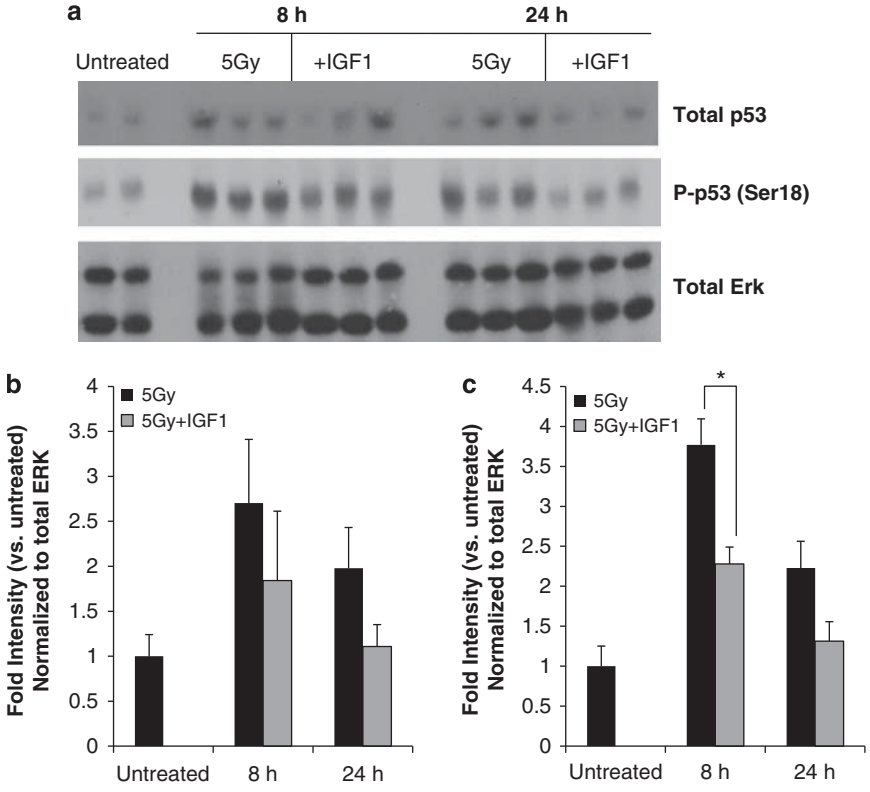

Figure 3 Parotid glands of irradiated mice pretreated with IGF1 have reduced levels of total and phosphorylated p53 protein. The head and neck regions of wild-type mice were irradiated ± IGF1 pretreatment. Parotid glands were removed, protein lysates were prepared, and western blotting was performed (**a**) as described in Materials and methods. Total ERK was used to confirm equal loading of lanes. (**b**, **c**) Blots were analyzed by densitometry, normalized to total Erk and shown as mean intensity relative to untreated + S.E.M. *A significant difference ($P \leqslant 0.05$) between irradiated glands ± IGF1 pretreatment as measured by a Student's *t*-test

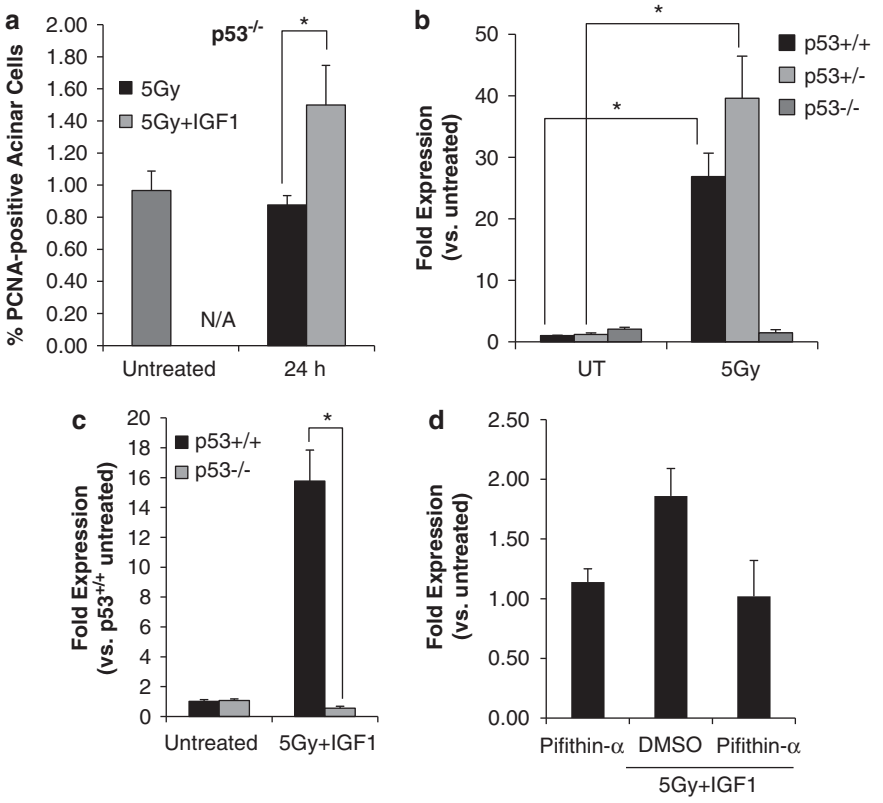

Figure 4 IGF1-induced cell cycle arrest in irradiated parotid glands is p53 dependent. The head and neck regions of wild-type ($p53^{+/+}$), $p53^{+/-}$ and $p53^{-/-}$ mice were irradiated (**a–c**). After 4, 8 and 24 h, parotid glands were removed. (**a**) In all, 24 h tissues were embedded in paraffin and stained for PCNA. The graphs represent the number of PCNA-positive acinar cells as a percentage of total acinar cells counted. The data are shown as the mean + S.E.M. of $\geqslant 3$ mice per treatment. *A significant difference ($P \leqslant 0.05$) between $p53^{+/+}$ and $p53^{-/-}$ glands as measured by a Student's *t*-test. (**b**, **c**) RNA was isolated after 4 (**b**) and 8 h (**c**), and real-time RT-PCR was run with primers to amplify p21. Results were calculated using the $2^{-\Delta\Delta C_t}$ method, normalized to wild-type untreated and shown as the mean + S.E.M. of $\geqslant 3$ mice per treatment. *A significant difference ($P \leqslant 0.05$) between untreated and irradiated glands of the same genotype (**b**) or irradiated glands ± IGF1 pretreatment (**c**). (**d**) Wild-type mice were treated interperitoneally with pifithrin-α (0.25 mg) for 12 h, then again immediately before IGF1 injection and head and neck irradiation. Parotid glands were removed after 8 h, RNA was isolated, and real-time RT-PCR was run with primers to amplify p21. Results were calculated using the $2^{-\Delta\Delta Ct}$ method, normalized to pifithrin-α alone and shown as the mean + S.D.

parotid glands, which occurs in wild-type animals, is p53 dependent.

Reduced levels of p63 in irradiated parotid glands pretreated with IGF1. An exact role for p63 in modulating DNA damage response is unknown; however, because of its ability to enhance or inhibit p53 transcriptional activity,[10] we chose to examine the effects of radiation on p63 expression in parotid glands. We performed RT-PCR for TAα, TAγ, ΔNα or ΔNγ to determine the isoforms expressed in salivary glands. The only detectable isoforms were ΔNα and ΔNγ (Figure 5a), which are also the only isoforms detectable by western blotting (Figure 5c).

Similarly to p53, p63 is affected by posttranslational modifications. A recent study showed that p63 is phosphorylated ($Ser^{66/68}$ in ΔN) in response to genotoxic stress, which may enhance its stability by reducing proteasomal degradation.[18] Levels of p63 in irradiated parotid glands were evaluated by real-time RT-PCR and western blotting for total and phosphorylated p63 ($Ser^{66/68}$). Radiation leads to a significant increase in p63 expression after 4 h as measured by real-time RT-PCR (Figure 5b). Increased transcription coincides with elevated total p63 protein after 8 and 24 h (Figure 5c). In contrast, pretreatment with IGF1 prevents increased p63 transcription after irradiation (Figure 5b). In addition, parotid glands from irradiated mice pretreated with IGF1 have reduced total p63 protein levels 8 and 24 h after treatment (Figure 5c). The same trend is observed when probing for phosphorylated p63 (Figure 5c), although reduction of phosphorylated p63 in the parotid glands of IGF1 pretreated mice 24 h after irradiation may simply be due to an overall reduction in p63 protein. These data indicate that acute radiation-induced increases in total and phosphorylated p63 are not maintained in parotid glands of irradiated mice pretreated with IGF1.

Reduced binding of ΔNp63 and increased binding of p53 to the p21 promoter in irradiated parotid glands pretreated with IGF1. The ΔN isoforms of p63 have been shown to function as transcriptional repressors *in vitro*, reducing expression of p53 target genes, such as p21, by binding to p53 response elements in their promoters.[11–13] Owing to increased p21 expression and G2/M arrest in irradiated mice pretreated with IGF1, we sought to determine

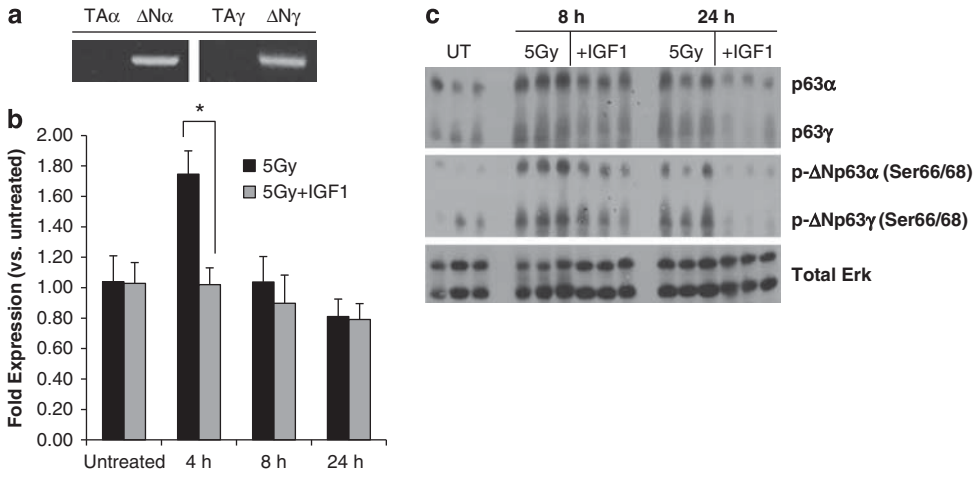

Figure 5 ΔNp63 mRNA and protein expression increases in irradiated parotid glands. (**a**) RNA was isolated from untreated parotid glands, and RT-PCR was run with primers to amplify p63 isoforms (TAα, ΔNα, TAγ and ΔNγ). PCR products were electrophoresed on a 1% agarose gel. (**b**) The head and neck regions of wild-type mice were irradiated ± IGF1 pretreatment. Parotid glands were removed, RNA was isolated and real-time RT-PCR was run with primers to amplify total p63. Results were calculated using the $2^{-\Delta\Delta C_t}$ method, normalized to untreated and shown as the mean + S.E.M. of ⩾3 mice per treatment. *A significant difference ($P \leqslant 0.05$) between irradiated glands ± IGF1 pretreatment as measured by a Student's *t*-test. (**c**) The head and neck regions of wild-type mice were irradiated ± IGF1 pretreatment. Parotid glands were removed, protein lysates were prepared and western blotting was performed as described in Materials and methods. Total ERK was used to confirm equal loading of lanes

the mechanism responsible using ChIP *in vivo* to evaluate relative binding of p53 and ΔNp63 to a p53 response element in the p21 promoter.

After 4 h, radiation has no effect on the amount ΔNp63 bound to the p21 promoter in parotid glands, regardless of whether or not mice were pretreated with IGF1 (Figure 6a). This coincides with equivalent p21 expression in the two groups of irradiated mice at that time-point (Figure 1d). After 8 h, binding of ΔNp63 to the p21 promoter increases in irradiated parotid glands, which is abrogated by pretreatment with IGF1 (Figure 6a). Using a p63α-specific antibody, we confirmed that ΔNα is capable of binding to the p21 promoter; however, p63γ-specific antibodies specific for immunoprecipitation are commercially unavailable. This IGF1-mediated reduction in binding of the transcriptional repressor ΔNp63 to the p21 promoter may account for increased p21 expression observed in this treatment group. A beads-only control using no antibody for IP was no different from untreated controls indicating that our pull-downs were specific (Figure 6b). The fold enrichments shown represent trends that were consistent between multiple independent experiments. The agarose gels shown with each graph were loaded with PCR-amplified input samples to show equal starting material for each IP.

We have shown that radiation-induced p21 expression is p53 dependent in parotid glands (Figure 4b) and that irradiated mice pretreated with IGF1 have sustained p21 expression (Figure 1d). Owing to decreased ΔNp63 binding to the p21 promoter in IGF1 pretreated glands (Figure 6a), we hypothesized a concomitant increase in p53 binding to the same response element. At both 4 and 8 h after irradiation, there is more p53 bound to the p21 promoter in the IGF1 pretreated group than in mice treated with radiation alone (Figure 7a). Similar to Figure 6b, a beads-only control was no different from untreated (Figure 7b). The fold enrichments shown represent trends that were consistent between multiple independent experiments. These data indicate that IGF1 may affect the ability of ΔNp63 to function as a competitive inhibitor to p53-induced transcription of p21 after irradiation.

IGF1-induced effects after irradiation are not detected in unstressed salivary glands. We have shown that IGF1 given immediately before irradiation reduces inhibitory binding of ΔNp63 to the p21 promoter, resulting in prolonged p21 gene expression and G2/M arrest. Generally, growth factors are thought to drive proliferation rather than induce cell cycle arrest. To test the hypothesis that IGF1 functions differently in irradiated glands than in unstressed glands, we repeated several of the experiments reported above in mice treated with IGF1 alone. Rather than increasing the percentage of G2/M cells as it did in irradiated glands, IGF1 increases the percentage of S-phase cells indicating an actively dividing population (Figure 8a). In parotid glands treated with IGF1, there is an increase in total p53 (Figure 8b) but because IGF1 does not initiate a DNA damage response, phosphorylation of p53 (Ser^{15}) is not observed (data not shown). IGF1 also induces total p63 and phosphorylated ΔNp63α ($Ser^{66/68}$) 8 and 24 h after injection (Figure 8b). Owing to the critical role of p63 in salivary gland development,[19,20] IGF1-induced proliferation may account for this response. Consistent with a role for IGF1 in driving proliferation in unstressed tissues, IGF1 alone does not induce transcription of the cell cycle inhibitor p21 (Figure 8c). This corresponds with increased binding of the transcriptional inhibitor ΔNp63 to the p21 promoter. Altogether, these results indicate that parotid glands stressed by radiation respond differently to IGF1 than unstressed glands.

Discussion

Radiation-induced loss of salivary function in patients treated for head and neck cancers is a severe morbidity that results in

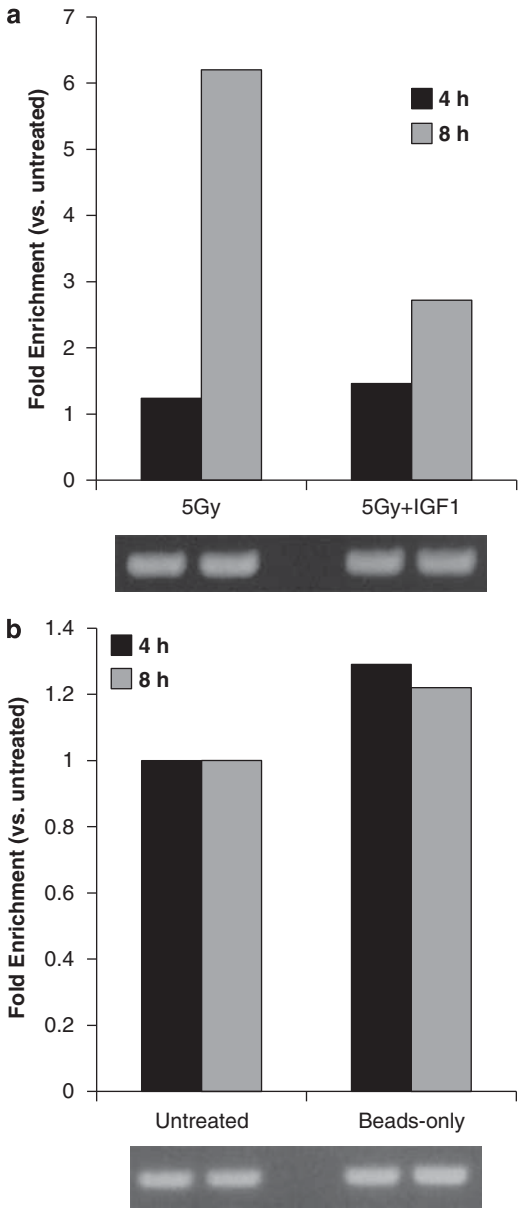

Figure 6 Binding of ΔNp63 to the p21 promoter is reduced in parotid glands of irradiated mice pretreated with IGF1. The head and neck regions of wild-type mice were irradiated ± IGF1 pretreatment. (**a**) ChIP was performed on parotid glands removed after 4 and 8 h with an antibody recognizing total p63. (**b**) ChIP was performed utilizing beads-only as a control. Precipitated DNA was analyzed by real-time PCR using primers for a region of the p21 promoter ~1390 bases upstream of the transcription start site. Results were calculated by normalizing the C_t value for each IP sample with the C_t value for its corresponding input (pre-IP chromatin) and calculating a ΔC_t. Normalized values are shown as fold *versus* untreated and represent trends that were consistent between multiple independent experiments. Agarose gels shown with each graph were loaded with PCR-amplified input samples to show equal starting material for each IP

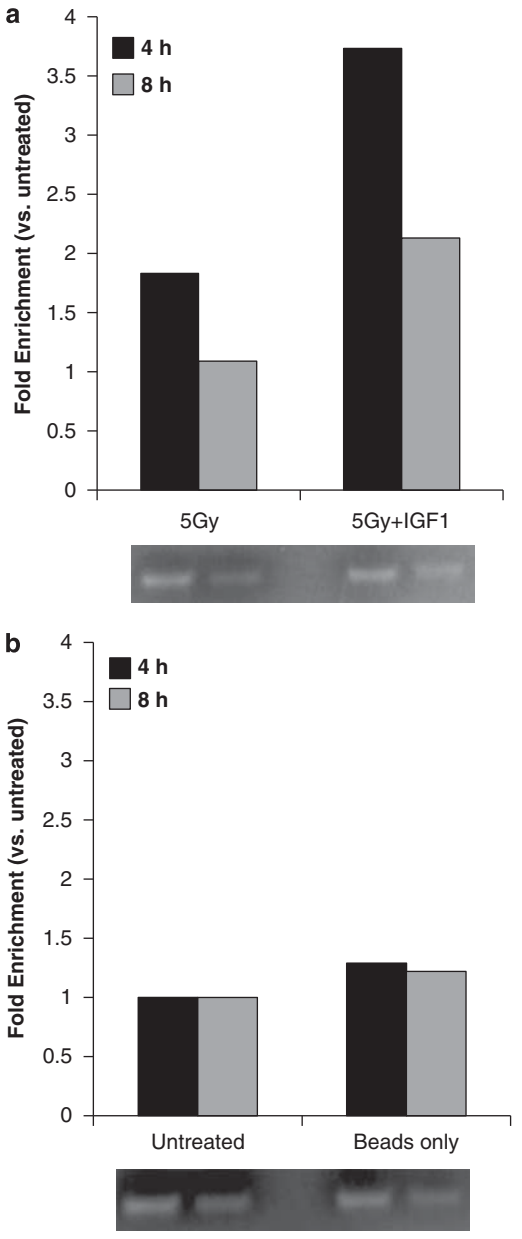

Figure 7 Binding of p53 to the p21 promoter is increased in parotid glands of irradiated mice pretreated with IGF1. The head and neck regions of wild-type mice were irradiated ± IGF1 pretreatment. (**a**) ChIP was performed on parotid glands removed after 4 and 8 h with an antibody recognizing total p53. (**b**) ChIP was performed utilizing beads-only as a control. Precipitated DNA was analyzed and graphed as described for Figure 6. Normalized values are shown as fold *versus* untreated and represent trends that were consistent between multiple independent experiments

chronic dry mouth, damaged oral mucosa, dysphagia and malnutrition.[2] Currently, therapy is limited to palliative treatment with muscarinic-cholinergic agonists, which stimulate secretion from remaining salivary cells. In addition to the lack of satisfactory functional results from these therapies, their nonspecific action produces a variety of side-effects, including nausea, diarrhea and excessive sweating. As a result of this, our research focuses on prevention of this damage.

In this study, we show that IGF1 elicits a different response in parotid glands stressed by radiation than it does in glands under normal conditions. Considerable evidence exists in the literature on the functions of IGF1 in unstressed environments, with the majority of *in vivo* studies indicating a role in cell and tissue hypertrophy (e.g., Stratikopoulos *et al*.[21]). Although studies in IGF1-null mice have indicated a role for

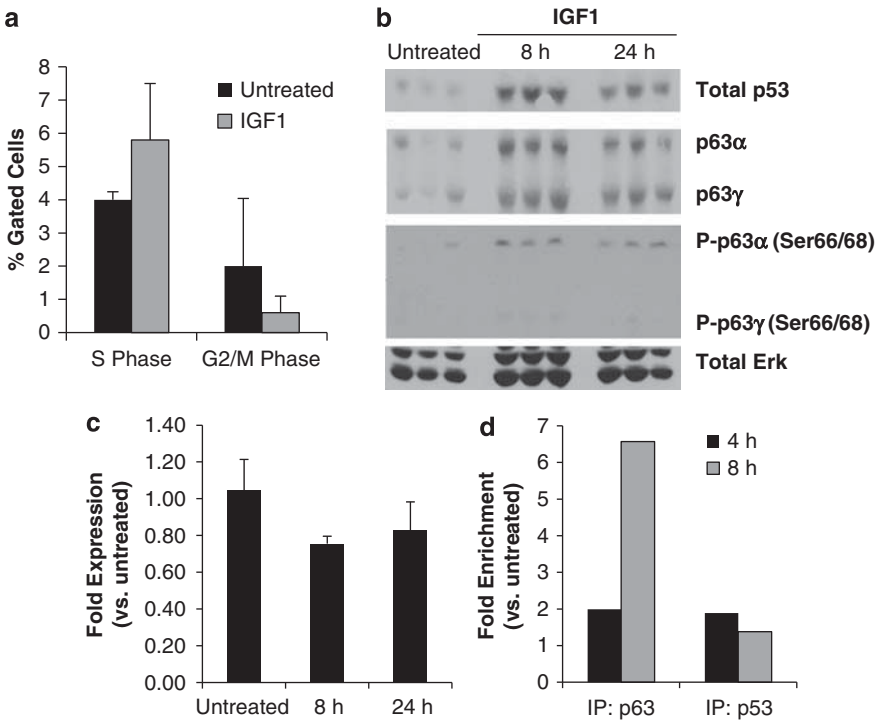

Figure 8 IGF1-induced effects after irradiation are not detected in unstressed salivary glands. Wild-type mice were treated with IGF1, and parotid glands were removed after 4, 8, and 24 h. (**a**) Cell cycle distribution was analyzed for 8 h tissues as described for Figure 1a. The data are shown as the mean percentage of gated cells in G2/M phase + S.E.M. of $\geqslant$3 mice per treatment. (**b**) In all, 8 and 24 h protein lysates were analyzed as described for Figure 3. (**c**) p21 mRNA expression was measured after 8 and 24 h as described for Figure 4. (**d**) ChIP was performed on 4 and 8 h tissues with an antibody recognizing total p63 or total p53. Precipitated DNA was analyzed and graphed as described for Figure 6. Normalized values are shown as fold *versus* untreated and represent trends that were consistent between multiple independent experiments

IGF1 in estradiol-induced G2 progression in the uterus,[22] few studies have investigated the effects of exogenous IGF1 on cell cycle progression *in vivo*. Our work uncovers a previously unnoticed effect of IGF1 in environments stressed by radiation. Specifically, we show that IGF1 induces a transient cell cycle arrest in irradiated glands, which does not occur with radiation alone (Figure 1).

Our previous work has established that attrition of salivary acinar cells to p53-dependent apoptosis is likely responsible for the side-effects observed after head and neck irradiation.[9,15,17] We hypothesize that cell cycle arrest in IGF1 pretreated mice facilitates DNA repair after irradiation, thereby impeding apoptosis. One study showed that inhibition of the DNA damage response by caffeine prevents G2/M arrest and triggers apoptosis in irradiated MCF-7 cells.[23] In osteosarcoma cells, inhibition of radiation-induced cell cycle arrest is a potent radiation sensitizer.[24] This is a plausible explanation for the sensitivity of salivary glands to radiation because there are no indications of cell cycle arrest in mice treated with radiation alone (Figure 1).

In salivary glands, IGF1 is a potent activator of the serine/threonine protein kinase Akt (protein kinase B) pathway.[16] It has been shown that constitutive activation of Akt1 (myr-Akt1) in primary murine salivary acinar cells results in reduced apoptosis after irradiation, which corresponds with decreased p53 phosphorylation at Ser[18].[17] Most importantly, modulation of the apoptotic response through activation of Akt (myr-Akt1 or a single intravenous dose of IGF1) correlates with preserved salivary gland function after a single dose of radiation.[15] Similar to IGF1 pretreated glands, transgenic mice expressing myr-Akt1 have enhanced G2/M arrest, reduced in proliferation and prolonged expression of p21 after irradiation (Figure 2). Pharmacological inhibition of Akt reduces the ability of IGF1 to upregulate p21 expression in response to radiation (Figure 2d), which suggests that IGF1-mediated cell cycle arrest may involve Akt.

In contrast to what has previously been shown in the literature, we indicate that IGF1 induces G2/M arrest after irradiation, ostensibly through transcriptional upregulation of p21 (Figure 1d). Mechanistically, we have shown that p21 promoter occupancy is different in parotid glands of IGF1 pretreated mice compared with parotid glands of mice treated with radiation alone. Specifically, we illustrate that radiation-induced increases in ΔNp63 protein correspond with enhanced binding to the p21 promoter and decreased p21 transcription in irradiated parotid glands after 8 h compared with parotid glands pretreated with IGF1 (Figures 1d, 5b and 6a, respectively). Our study concurs with a previously suggested role for ΔNp63 in mitigating DNA damage-induced p21 expression[12] and has extended this observation to *in vivo*. Although slight differences in DNA binding sites make promoters more selective for a specific p53 family member,[25] inhibition of p53 target genes by ΔNp63 may be due to competitive binding to these sites. Supporting this hypothesis,

we show that there is an inverse relationship between p53 and ΔNp63 binding to the p21 promoter in the salivary glands of mice pretreated with IGF1 before irradiation (Figure 7a). Particularly, we show that in spite of the elevated levels of p53 protein in irradiated glands (Figure 3), binding of p53 to the p21 promoter decreases along with p21 transcription (Figures 3 and 7a). Taken together, these data suggest that in parotid glands of irradiated mice pretreated with IGF1, reduced ΔNp63 protein facilitates a p53-mediated increase in p21 expression leading to G2/M arrest.

It is well established that DNA damage results in stabilization and increased transcriptional activity of p53;[7] however, the genes transcribed by p53 include both pro-apoptotic and cell cycle arrest genes. Our data indicate that competitive binding of ΔNp63 to p53 response elements in the p21 promoter may direct p53 to other promoters, thereby accounting for selective activation of p53 target genes and initiation of a cell death or cell cycle arrest program. In non-diseased salivary glands, suppression of apoptosis by IGF1 results in a positive clinical output – the long-term preservation of salivary function.[15] These results provide the basis for rational design of small molecule inhibitors to prevent radiation-induced attrition of salivary cells. The need for this is urgent because there are currently no satisfactory methods to protect or restore salivary gland function after radiation therapy.

Materials and Methods

Mice. All experiments were conducted in 4- to 5-week-old FVB females. For p53 knockout experiments, mice were provided by Dr. Carla van den Berg (University of Texas, Austin, TX, USA) on a Balb/c background and back-crossed to FVB for 11 generations. For myr-Akt1 experiments, FVB mice expressing the myr-Akt1 transgene under control of the mouse mammary tumor virus promoter were generated at the University of Colorado Health Sciences Center. The salivary gland phenotype was described previously.[17] Genotyping of transgenic mice was conducted as previously described[17,26] using PCR primers from integrated DNA technology (IDT, Coralville, IA, USA). All mice were maintained and treated in accordance with protocols approved by the University of Arizona Institutional Animal Care and Use Committee.

Treatment. Mice were treated with radiation, intravenous IGF1 or a combination of the two. For irradiation, mice were anesthetized with avertin (0.4–0.6 mg/kg) and subjected to 5 Gy of targeted head and neck irradiation (^{60}Co therapeutic irradiator, Theratron-80, Atomic Energy of Canada Ltd, Ottawa, Canada) as previously described.[9] Mice treated with IGF1 received 5 μg of intravenous recombinant human IGF1 (GroPrep, Adelaide, Australia) as previously described.[15] For those mice that received the combination treatment, IGF1 injections occurred immediately before irradiating the animal. For pifithrin-α experiments, mice were treated intraperitoneally with 0.25 mg (in 100 μl of DMSO) of pifithrin-α (cyclic, hydrobromide, Enzo Life Sciences, Plymouth Meeting, PA, USA) twice – 12 h before, then immediately before IGF1 injections and irradiation. For deguelin experiments, mice were treated interperitoneally with 4 mg/kg (in $<$100 μl of DMSO) of deguelin (Enzo Life Sciences) immediately before IGF1 injections and irradiation.

Flow cytometry. Pairs of glands were minced in dispersion media,[27] mixed at 37 °C for 20 min, resuspended in modified Hank's media with 1 μM EGTA, and mixed again at 37 °C for 10 min. Tissue was disrupted by pipette and filtered through 20 μm mesh. This single cell suspension was centrifuged ($\sim 100 \times g \times$ 10 min) 2 $\times$ in cold PBS and fixed by adding 500 μl of 100% ethanol. After storing at -20 °C overnight, cells were centrifuged ($\sim 100 \times g \times 15$ min), resuspended in 462.5 μl of cold PBS and incubated at 37 °C for 30 min with 25 μl of RNase A (10 mg/ml, Invitrogen, Carlsbad, CA, USA) and 12.5 μl of propidium iodide (1.6 mg/ml, MP Biomedicals, Solon, OH, USA). Cell cycle distribution was measured by the AZCC/ARL Division of Biotechnology Cytometry Core Facility using a FACScan flow cytometer (BD Biosciences, San Jose, CA, USA) and analyzed using CellQuest Pro software (BD Biosciences).

PCNA staining. Glands were fixed overnight in 10% neutral buffered formalin, transferred to 70% ethanol and embedded in paraffin. Tissues were cut into 4 μm sections by the Histology Service Laboratory in the Department of Cell Biology and Anatomy at the University of Arizona, Tucson, AZ, USA. Slides were stained for PCNA (Santa Cruz Biotechnology, Santa Cruz, CA, USA). Briefly, slides were heated to 37 °C for 30 min and rehydrated in histoclear, graded alcohols and distilled water. Nonspecific peroxidase activity was quenched with 0.3% H_2O_2. For antigen retrieval, slides were placed in citrate buffer (pH 6.0), heated twice in a microwave for 5 min and allowed to cool. After washes, slides were treated as instructed by the manufacturer (Vectastain Elite ABC kit, PK-6101, Vector Laboratories, Burlingame, CA, USA). Color development was performed using Biogenex (San Ramon, CA, USA) DAB incubation for 6–8 min. Slides were counterstained with Gill's hematoxylin, dehydrated and mounted in Permount (Thermo Fisher Scientific, Pittsburg, PA, USA). Images were made with a Leica DM5500 (Leica Microsystems, Wetzlar, Germany) and 4 megapixel Pursuit camera (Diagnostic Instruments, Inc, Sterling Heights, MI, USA). PCNA-positive acinar cells in parotid sections were counted from a minimum of three fields of view per slide from three slides per treatment (three mice).

Western blotting. Glands were homogenized in RIPA[17] supplemented with SIGMAFAST protease inhibitor cocktail (Sigma-Aldrich, St Louis, MO, USA) and 5 mM sodium orthovanadate. After adding 100 μg/ml of PMSF, samples were boiled for 10 min and sonicated until homogenous. Protein concentrations were determined using Coomassie Plus Protein Assay Reagent (Thermo Fisher Scientific). In all, 100 μg of each sample was loaded on an 8% polyacrylamide gel, transferred to a 0.45 μm Immobilon-P membrane (Millepore, Bedford, MA, USA), and immunoblotted with one of the following antibodies: anti-ERK (Promega, Madison, WI, USA), anti-p53 (DO-1, Santa Cruz Biotechnology), anti-phosphorylated p53 (Ser^{15}) (Cell Signaling Technologies, CST, Beverly, MA, USA), anti-p63 (4A4, Abcam, Cambridge, MA, USA), anti-phosphorylated p63 (Ser$^{66/68}$ in human ΔNp63) (CST), anti-phosphorylated cdc2 (Tyr^{15}) (Santa Cruz Biotechnology), anti-cdc2 (Calbiochem/EMD, Gibbstown, NJ, USA), anti-cdc25a (CST) and anti-p21 (Santa Cruz Biotechnology). Secondary antibodies were conjugated with HRP (goat anti-mouse and goat anti-rabbit, Bio-Rad, Hercules, CA, USA; anti-mouse TrueBlot for anti-p63 and anti-phosphorylated p63 primaries, eBioscience, San Diego, CA, USA; anti-goat for anti-phosphorylated cdc2, Santa Cruz Biotechnology), and ECL substrate (Thermo Fisher Scientific) was used for detection as instructed by the manufacturer. Membranes were stripped with restore western blot stripping buffer (Thermo Fisher Scientific), reblocked and reprobed as previously described.[17] Densitometry was analyzed using ImageJ (NIH, Bethesda, MD, USA), normalized to total ERK and shown as mean intensity relative to untreated.

RNA Isolation and RT-PCR. RNA was isolated as previously described[17] and quantified. In all, 1 μg of RNA was reverse transcribed using a Super Script III Kit as instructed by the manufacturer (Invitrogen) and diluted 1 : 5 for subsequent analysis (PCR and gel electrophoresis or real-time PCR).

PCR and gel electrophoresis. Diluted cDNA was amplified using AccuPower HotStart PCR PreMix with specific primers as instructed by the manufacturer (Bioneer, Alameda, CA, USA). The following primers were purchased from IDT: TAp63 forward: 5′-ATGTCGCAGAGCACCCAG-3′, ΔNp63 forward: 5′-CCAGACTCAATTTAGTGAGCCAC-3′, p63α reverse: 5′-ACAACCTTGCTAAG AAAACTGA-3′, p63γ reverse: 5′-CTCCACAAGCTCATTCCTGAAGC-3′. Products were run on a 1% agarose gel.

Real-time PCR. The following real-time reaction mix was prepared: 5 μl of diluted cDNA, 1 μl of mixed forward and reverse primers (10 μM each), 12.5 μl of SYBR Green (Qiagen, Alameda, CA, USA), and nuclease-free water to a final volume of 25 μl. Reactions were using an iQ5 Real-Time PCR Detection System (Bio-Rad) and analyzed as previously described.[9] Normalized values were plotted as relative fold over untreated. The following primers were purchased from IDT: S15,[17] p21,[17] total p63 forward: 5′-CGTCCAATTTTAATCATCGTTAC-3′, total p63 reverse: 5′-CTGTCTTCATCTGCCTTCC-3′. QuantiTect primer for mouse IGF1 was purchased from Qiagen.

Chromatin immunoprecipitation. Glands were fixed in 1.5% paraformaldehyde for 10 min, washed twice with cold PBS and resuspended in 750 μl of RIPA (50 mM Tris-HCl (pH 8), 150 mM NaCl, 2 mM EDTA (pH 8), 1% NP-40, 0.5% sodium

deoxycholate and 0.1% SDS) supplemented with SIGMAFAST protease inhibitor cocktail (Sigma-Aldrich). After homogenizing, samples were sonicated eight times for 15 s at power = 2.0 using a Sonicator 3000 (Misonix, Farmingdale, NY, USA) to yield ~1 kb DNA fragments. In all, 50 μl of each chromatin sample was added to 70 μl of elution buffer (1% SDS and 100 mM sodium bicarbonate in PBS) with 10 μl of proteinase K (10 mg/ml, Thermo Fisher Scientific) and incubated overnight at 65 °C. DNA was purified using a QIAquick PCR purification kit (Qiagen) as instructed by the manufacturer, eluted in 30 μl, and quantified. DNA was diluted to equal concentrations in DEPC water and set aside as the input fraction. Chromatin samples were diluted in RIPA to ensure equal starting material (~15 μg of DNA) for subsequent IPs. Samples were cleared by incubating with 30 μl of protein A/G agarose beads (Thermo Fisher Scientific) for 1 h at 4 °C. In another tube, 30 μl of protein A/G agarose beads were incubated in RIPA with 2 μg of sheared salmon sperm DNA (Invitrogen), and 3 μl of 1% BSA for 2 h at room temperature. After centrifuging and removing the beads from the cleared IP samples, the pre-absorbed beads were added along with 3 μg of antibody (total p63: mouse monoclonal (4A4), Abcam; p63α: rabbit monoclonal (H-129), Santa Cruz; p53: rabbit polyclonal (FL-393), Santa Cruz Biotechnology) and incubated overnight at 4 °C. Beads were washed three times with wash buffer (150 mM NaCl, 20 mM Tris-HCl (ph 8), 2 mM EDTA, 1% Triton X-100 and 0.1% SDS), once with final wash buffer (wash buffer with 500 mM NaCl), and resuspended in 120 μl of elution buffer. After 15 min, 10 μl of proteinase K (10 mg/ml) was added, and samples were incubated overnight at 65 °C. IP DNA was purified in the same way as input DNA. For quantification, equal volumes of DNA from each IP and input sample were amplified by real-time PCR (following the protocol described above) using primers for a region of the p21 promoter that is ~1390 bases upstream of the transcription start site (IDT, forward: 5′-TCTTGCTATGTAGCCCATGT-3′, reverse: 5′-TACGGATGTTCCTGACAGAC-3′). Results were calculated by normalizing the C_t value for each IP sample with the C_t value for its corresponding input (pre-IP chromatin) and calculating a ΔC_t. Normalized values were graphed as fold over untreated. To confirm equal starting material for each IP, input DNA was amplified using the p21 promoter primers and run on a 1% agarose gel (see PCR and gel electrophoresis protocol above).

Statistical analysis. Single comparisons were made between two groups using Student's *t*-tests calculated with Microsoft Excel.

Conflict of interest

GCM, JLF, SS, JLA and RB have no conflict of interest to report. KHL is listed as an inventor on US Patent Application No. 12/304,359.

Acknowledgements. We thank Junesse Farley at the AZCC/ARL Division of Biotechnology Cytometry Core Facility for her technical help. GCM was supported by an NSF GK-12 fellowship (NSF 0338247) and an NCI institutional training grant fellowship (T32 CA09213). KHL was supported by an NIDCR K22 (DE16096) and an R01 (DE18888). The funders had no role in study design, data collection and analysis, decision to publish or preparation of the paper.

1. Jemal A, Siegel R, Ward E, Hao Y, Xu J, Thun MJ. Cancer statistics, 2009. *CA Cancer J Clin* 2009; **59**: 225–249.
2. Grundmann O, Mitchell GC, Limesand KH. Sensitivity of salivary glands to radiation: from animal models to therapies. *J Dent Res* 2009; **88**: 894–903.
3. Eisbruch A, Ten Haken RK, Kim HM, Marsh LH, Ship JA. Dose, volume, and function relationships in parotid salivary glands following conformal and intensity-modulated irradiation of head and neck cancer. *Int J Radiat Oncol Biol Phys* 1999; **45**: 577–587.
4. Banin S, Moyal L, Shieh S, Taya Y, Anderson CW, Chessa L *et al.* Enhanced phosphorylation of p53 by ATM in response to DNA damage. *Science* 1998; **281**: 1674–1677.
5. Canman CE, Lim DS, Cimprich KA, Taya Y, Tamai K, Sakaguchi K *et al.* Activation of the ATM kinase by ionizing radiation and phosphorylation of p53. *Science* 1998; **281**: 1677–1679.
6. Tibbetts RS, Brumbaugh KM, Williams JM, Sarkaria JN, Cliby WA, Shieh SY *et al.* A role for ATR in the DNA damage-induced phosphorylation of p53. *Genes Dev* 1999; **13**: 152–157.
7. Woods DB, Vousden KH. Regulation of p53 function. *Exp Cell Res* 2001; **264**: 56–66.
8. Gudkov AV, Komarova EA. The role of p53 in determining sensitivity to radiotherapy. *Nat Rev Cancer* 2003; **3**: 117–129.
9. Avila JL, Grundmann O, Burd R, Limesand KH. Radiation-induced salivary gland dysfunction results from p53-dependent apoptosis. *Int J Radiat Oncol Biol Phys* 2009; **73**: 523–529.
10. Yang A, Kaghad M, Wang Y, Gillett E, Fleming MD, Dötsch V *et al.* p63, a p53 homolog at 3q27–29, encodes multiple products with transactivating, death-inducing, and dominant-negative activities. *Mol Cell* 1998; **2**: 305–316.
11. Barbieri CE, Perez CA, Johnson KN, Ely KA, Billheimer D, Pietenpol JA. IGFBP-3 is a direct target of transcriptional regulation by DeltaNp63alpha in squamous epithelium. *Cancer Res* 2005; **65**: 2314–2320.
12. Schavolt KL, Pietenpol JA. p53 And delta Np63 alpha differentially bind and regulate target genes involved in cell cycle arrest, DNA repair and apoptosis. *Oncogene* 2007; **26**: 6125–6132.
13. Westfall MD, Mays DJ, Sniezek JC, Pietenpol JA. The delta Np63 alpha phosphoprotein binds the p21 and 14-3-3 sigma promoters *in vivo* and has transcriptional repressor activity that is reduced by Hay-Wells syndrome-derived mutations. *Mol Cell Biol* 2003; **23**: 2264–2276.
14. Bunz F, Dutriaux A, Lengauer C, Waldman T, Zhou S, Brown JP *et al.* Requirement for p53 and p21 to sustain G2 arrest after DNA damage. *Science* 1998; **282**: 1497–1501.
15. Limesand KH, Said S, Anderson SM. Suppression of radiation-induced salivary gland dysfunction by IGF-1. *PLoS One* 2009; **4**: e4663.
16. Limesand KH, Barzen KA, Quissell DO, Anderson SM. Synergistic suppression of apoptosis in salivary acinar cells by IGF1 and EGF. *Cell Death Differ* 2003; **10**: 345–355.
17. Limesand KH, Schwertfeger KL, Anderson SM. MDM2 is required for suppression of apoptosis by activated Akt1 in salivary acinar cells. *Mol Cell Biol* 2006; **26**: 8840–8856.
18. Petitjean A, Ruptier C, Tribollet V, Hautefeuille A, Chardon F, Cavard C *et al.* Properties of the six isoforms of p63: p53-like regulation in response to genotoxic stress and cross talk with DeltaNp73. *Carcinogenesis* 2008; **29**: 273–281.
19. Yang A, Schweitzer R, Sun D, Kaghad M, Walker N, Bronson RT *et al.* p63 is essential for regenerative proliferation in limb, craniofacial and epithelial development. *Nature* 1999; **398**: 714–718.
20. Mills AA, Zheng B, Wang XJ, Vogel H, Roop DR, Bradley A. p63 Is a p53 homologue required for limb and epidermal morphogenesis. *Nature* 1999; **398**: 708–713.
21. Stratikopoulos E, Szabolcs M, Dragatsis I, Klinakis A, Efstratiadis A. The hormonal action of IGF1 in postnatal mouse growth. *Proc Natl Acad Sci USA* 2008; **105**: 19378–19383.
22. Adesanya OO, Zhou J, Samathanam C, Powell-Braxton L, Bondy CA. Insulin-like growth factor 1 is required for G2 progression in the estradiol-induced mitotic cycle. *Proc Natl Acad Sci USA* 1999; **96**: 3287–3291.
23. Wendt J, Radetzki S, von Haefen C, Hemmati PG, Güner D, Schulze-Osthoff K *et al.* Induction of p21CIP/WAF-1 and G2 arrest by ionizing irradiation impedes caspase-3-mediated apoptosis in human carcinoma cells. *Oncogene* 2006; **25**: 972–980.
24. Syljuåsen RG, Sørensen CS, Nylandsted J, Lukas C, Lukas J, Bartek J. Inhibition of Chk1 by CEP-3891 accelerates mitotic nuclear fragmentation in response to ionizing radiation. *Cancer Res* 2004; **64**: 9035–9040.
25. Perez CA, Ott J, Mays DJ, Pietenpol JA. p63 Consensus DNA-binding site: identification, analysis and application into a p63MH algorithm. *Oncogene* 2007; **26**: 7363–7370.
26. Kuperwasser C, Hurlbut GD, Kittrell FS, Dickinson ES, Laucirica R, Medina D *et al.* Development of spontaneous mammary tumors in BALB/c p53 heterozygous mice. A model for Li-Fraumeni syndrome. *Am J Pathol* 2000; **157**: 2151–2159.
27. Quissell DO, Redman RS, Mark MR. Short-term primary culture of acinar-intercalated duct complexes from rat submandibular glands. *In Vitro Cell Dev Biol* 1986; **22**: 469–480.